

## Origin of Ultralow Friction and Wear in Ultrananocrystalline Diamond

A. R. Konicek,<sup>1</sup> D. S. Grierson,<sup>2</sup> P. U. P. A. Gilbert,<sup>3,\*</sup> W. G. Sawyer,<sup>4</sup> A. V. Sumant,<sup>5</sup> and R. W. Carpick<sup>6</sup>

<sup>1</sup>*Department of Physics & Astronomy, University of Pennsylvania, Philadelphia, Pennsylvania, 19104, USA*

<sup>2</sup>*Department of Engineering Physics, University of Wisconsin-Madison, Madison, Wisconsin, 53706, USA*

<sup>3</sup>*Department of Physics, University of Wisconsin-Madison, Madison, Wisconsin, 53706, USA*

<sup>4</sup>*Department of Mechanical and Aerospace Engineering, University of Florida, Gainesville, Florida, 32611, USA*

<sup>5</sup>*Center for Nanoscale Materials, Argonne National Laboratory, Argonne, Illinois, 60439, USA*

<sup>6</sup>*Department of Mechanical Engineering and Applied Mechanics, University of Pennsylvania, Philadelphia, Pennsylvania, 19104, USA*

(Received 16 October 2007; published 11 June 2008)

The impressively low friction and wear of diamond in humid environments is debated to originate from either the stability of the passivated diamond surface or sliding-induced graphitization/rehybridization of carbon. We find ultralow friction and wear for ultrananocrystalline diamond surfaces even in dry environments, and observe negligible rehybridization except for a modest, submonolayer amount under the most severe conditions (high load, low humidity). This supports the passivation hypothesis, and establishes a new regime of exceptionally low friction and wear for diamond.

DOI: [10.1103/PhysRevLett.100.235502](https://doi.org/10.1103/PhysRevLett.100.235502)

PACS numbers: 81.40.Pq, 46.55.+d, 62.20.Qp

The remarkably low friction and wear of diamond, particularly in humid environments, is postulated to be due to either rehybridization [1–3], or passivation [4,5] of dangling bonds formed during sliding. Rehybridization to ordered  $sp^2$  bonding is plausible because graphite is the thermodynamically stable form of carbon at room temperature and ambient pressure, and is lubricious due to its layered structure. Rehybridization may also involve the formation of lubricious amorphous  $sp^2$ -containing carbon [6]. The significant energy barrier to convert diamond to graphite or amorphous carbon ( $\sim 1.0$  eV/atom) [7] may be lowered by shear, frictional heating, and oxygen and water vapor. However, passivation is proposed by others [4,5,8] because friction and wear for diamond are lower, compared to vacuum, in environments containing  $H_2$  or  $H_2O$ . Desorption, induced mechanically, creates dangling carbon bonds that increase friction and wear due to interfacial bonding [9]. A sufficient supply of passivating species overcomes this by preemptively terminating the dangling bonds. However, no previous studies presented spectroscopic evidence to validate either hypothesis.

Ultrananocrystalline diamond (UNCD), one of the smoothest diamond films available, has a thickness-independent RMS roughness of  $<12$  nm over a  $1 \mu m^2$  area [10]. UNCD has equiaxed diamond grains  $\sim 2$ – $5$  nm in diameter with atomically abrupt grain boundaries, and shares many of the properties of diamond [11,12]. UNCD films  $\sim 1 \mu m$  thick were deposited onto silicon flats and  $Si_3N_4$  spheres [13]. Substrates were ultrasonically pretreated as in [10] except with functionalized nanodiamond powder ( $\sim 4$  nm diameter; ITC, Inc., Raleigh, NC) in dimethylsulfoxide before UNCD growth. We conducted four tribology experiments with UNCD sliding against UNCD, varying relative humidity (RH) and load. We determined the hybridization and chemistry after sliding by analyzing wear tracks and unworn regions using x-ray

photoelectron emission microscopy (X-PEEM) with near-edge x-ray absorption fine structure (NEXAFS) spectroscopy [14,15]. At the carbon edge, this technique is sensitive to the top  $\sim 3$  nm of the surface [16]. We have previously shown that X-PEEM can differentiate between worn and unworn UNCD regions, with high sensitivity to hybridization and chemistry [17].

Friction tests were performed with a microtribometer in an environmental chamber [18,19]. We produced four wear tracks on one UNCD flat by reciprocating sliding in an Ar atmosphere [20], using either 0.1 or 1.0 N load (initial mean Hertzian contact pressures 300 and 649 MPa, respectively) and either 1.0% or 50% RH. A new sphere was used for each track. The tracks are hereafter referred to as *HD*, *LD*, *HW*, and *LW*, signifying load (*High* or *Low*) and humidity (*Dry* or *Wet*), respectively.

To find the wear volume removed for each track, we performed optical profilometry measurements [21]. We calculated the wear rate of the film on the substrate using Archard's law [22].

While initial friction coefficients were different (Fig. 1 and Table I), the steady-state friction coefficients for all tests were approximately the same ( $\sim 0.02$ ) [23]. Previously, the lowest friction coefficient ever measured for diamond in dry conditions was 0.03–0.04, for a fine-grained diamond film in contact with a bulk diamond pin in dry  $N_2$  [24].

Tracks *HW*, *LD*, and *LW* all exhibited similarly excellent friction behavior. For the *HD* track, the nominal contact area grew significantly as the interface evolved, as evidenced by its larger track width ( $\sim 195 \mu m$ ). The low friction behavior occurring after the significant run-in period may be associated with a reduced average contact pressure. The trends observed suggest that a low friction coefficient is achievable with UNCD at any  $RH \geq 1.0\%$  if the contact pressure is below a critical value.

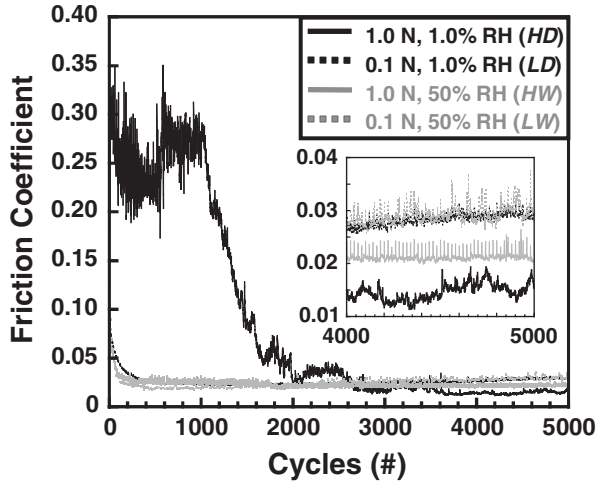


FIG. 1. Friction data from four wear tracks made with either 1.0 N (solid line) or 0.1 N (dashed line) load, and 1.0% (black line) or 50% (gray line) RH. (inset) Zoom of the last 1000 cycles showing low, steady-state friction. The two dashed curves fall on top of one another.

We collected Raman spectra from the spheres both inside and outside of the wear scars immediately after each track was made [25]. The spectra from inside the wear scars were indistinguishable from the unworn UNCD flat and identical to previously reported spectra [26]. This spectroscopy showed the films on the spheres did not wear through.

The steady-state friction coefficients  $\mu_{ss}$  and global wear rates are reported in Table I. According to profilometry, only track *HD* exhibited significant topographic modification. The wear scar depth was greater than 4  $\mu\text{m}$ , much deeper than the 1  $\mu\text{m}$  thickness of the coating. Spectroscopy and cross-sectional transmission electron microscopy confirmed that the coating was still present within the wear track, indicating the Si substrate was irreversibly compressed. This pronounced depression was not observed with track *HW*, even though the load was the same. Pronounced debris also demonstrates that track *HD* wore at a higher rate, presumably due to the high friction run-in period. The other wear rates are similar to or less than those for smooth nanocrystalline diamond films [24,27].

We extracted NEXAFS spectra from each track [28]. Division maps (image ratios at energies on and off spectral

peaks) enhance chemical contrast and were used to define the regions for analysis. A region with the strongest intensity at 285 eV is drawn on an X-PEEM image obtained at 289 eV [Fig. 2(a)] completely inside track *HD*.

For unworn UNCD, the small peak at 285 eV is due to the C  $1s \rightarrow \pi^*$  transition for disordered carbon-carbon bonds. This peak directly correlates with the amount of  $sp^2$ -bonded carbon ( $\sim 5\%$ , as in all UNCD films [11]) in the sampled region due to the surface contamination, reconstruction, and grain boundaries. The edge jump at  $\sim 289$  eV, the exciton peak at  $\sim 289.3$  eV, and the second band gap at 302.5 eV are due to the C  $1s \rightarrow \sigma^*$  transition for ordered  $sp^3$ -hybridized carbon-carbon bonds [29].

The C  $1s$  spectra extracted from worn regions are very similar to those of unworn UNCD, even for the *HD* track [Fig. 2(b)], with no observable rehybridization for the *LD*, *LW*, and *HW* tracks. For visualization only, the spectra shown are normalized to set the preedge to zero and the postedge at 320 eV to one. All quantitative analysis is based on relative areas of specified energy windows with respect to the postedge intensity from 289–325 eV within single spectra. There is some conversion to  $sp^2$ -bonded carbon in the representative image of the *HD* track [Fig. 2(a)], evident from the increased intensity at 285 eV ( $sp^2$  content is 21% in the drawn region, 18% averaged over the entire image). None of the C  $1s \rightarrow \pi^*$  peaks exhibit the shift from 285 to 285.5 eV that occurs for ordered graphite [30,31].

Surface passivation by H or O is typically manifested in C  $1s$  spectra as increased intensity from 286–289 eV [inset of Fig. 2(b)]. This is because the C=O bond is at  $\sim 286.4$  eV [29,31] and the C—H bond is at  $\sim 287.5$  eV on diamond [29]. We indeed find that the tracks exhibit small to significant increases in spectral intensity in this energy window of  $\sim 14\%$ ,  $\sim 140\%$ ,  $\sim 69\%$ , and  $\sim 205\%$  compared to unworn UNCD for the most heavily modified areas of *LW*, *HW*, *LD*, and *HD* tracks, respectively. We do not claim that this corresponds to the instantaneous chemistry present during sliding, but rather that in the worn region: (a) ordered graphite is not formed since it would not disappear upon ambient exposure; and (b) oxidized species indicate that dangling bonds were produced and eventually passivated. Given the rapid dissociation times and highly favorable energetics of water dissociation on the diamond dangling bonds [32] passivation likely occurred during sliding. Chemical modifications can occur

TABLE I. The contact conditions, respective track labels, steady-state friction coefficient ( $\mu_{ss}$ ) found by averaging the last 1000 cycles, number of run-in cycles, final track width, and global wear rate for each track. The total number of cycles was 5000 for all conditions. The wear rate for the *HD* track is an upper bound due to the extreme geometry of the wear scar.

Contact conditions	Label	$\mu_{ss}$	No. of run-in cycles	Track width ( $\mu\text{m}$ )	Wear rate ( $\text{mm}^3 \text{N}^{-1} \text{m}^{-1}$ )
1.0 N load 1.0% RH	<i>HD</i>	$0.015 \pm 0.002$	2000	195	$\ll 3 \times 10^{-5}$
0.1 N load 1.0% RH	<i>LD</i>	$0.028 \pm 0.001$	<500	40	$1.2 \times 10^{-7}$
1.0 N load 50% RH	<i>HW</i>	$0.0212 \pm 0.0008$	<250	55	$3.9 \times 10^{-10}$
0.1 N load 50% RH	<i>LW</i>	$0.029 \pm 0.002$	<250	25	$<2.5 \times 10^{-10}$

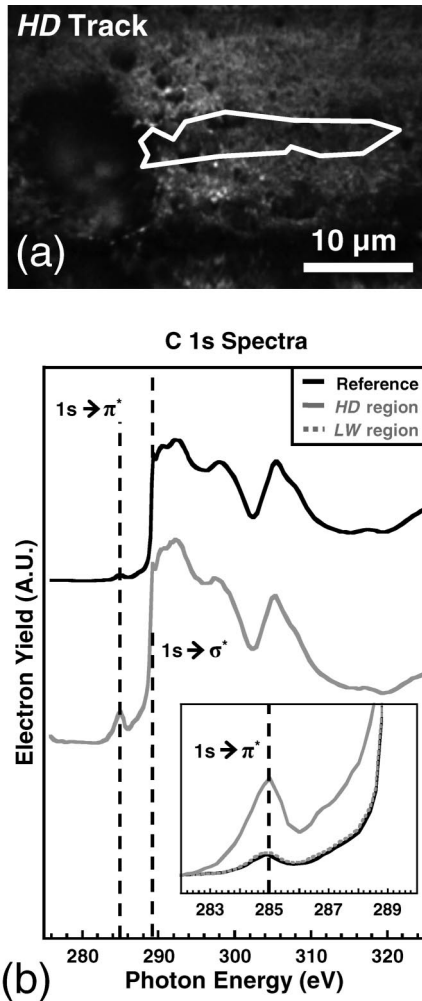


FIG. 2. (a) X-PEEM image at 289 eV inside the *HD* track. (b) C 1s spectra, offset for clarity. The top spectrum (black line) is a reference taken far from the wear track, and the bottom spectrum (gray line) is from the region drawn in (a). Inset: magnified plot of the spectra from (b) and a spectrum from track *LW*, in the  $1s \rightarrow \pi^*$  region.

afterward, but *differences* between worn and unworn regions show that tribochemical changes occurred.

To further rule out the formation of graphite, we used the transmission properties of x-rays through graphite and diamond and the electron emission properties of carbon [33] to simulate a NEXAFS spectrum for one monolayer of graphite on top of UNCD (Fig. 3, solid gray line). This methodology will be described in full detail elsewhere. Briefly, atomic densities were used to determine the penetration depth of x-rays, and the known spacing between graphite planes was used as the monolayer thickness. For this hypothetical structure,  $\sim 27\%$  of the electrons emitted at the C *K* edge come from the monolayer. Thus, the simulated spectrum is the linear combination of 27% graphite and 73% UNCD. The  $sp^2$  percentage determined here is a lower bound since the monolayer thickness was a lower bound, we assumed the longest electron mean inelastic path for carbon (7.5 Å), and interlayer bonding

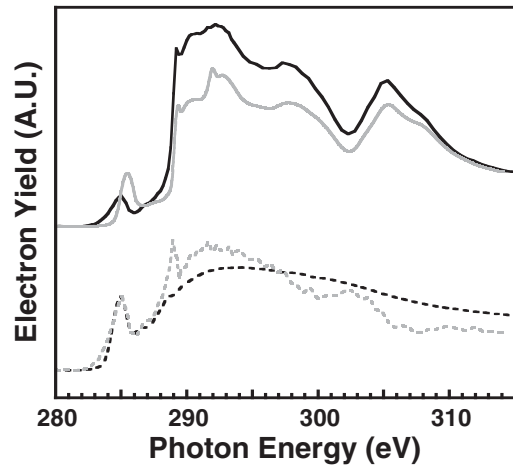


FIG. 3. A comparison of NEXAFS spectra. Top: experimental data from the most heavily worn region of the *HD* wear track (solid black line) and a simulation for one monolayer of graphite on UNCD (solid gray line). Bottom: spectrum from hydrogenated amorphous carbon (dashed black line) and subtraction of an unworn UNCD spectrum from the *HD* track spectrum (dashed gray line).

(with possible  $sp^2$  character) was ignored. A simulated spectrum with the same  $sp^2$  content as the most heavily modified region of track *HD* corresponds to a coverage of only  $42 \pm 2\%$  of a monolayer of graphite. Further evidence for the lack of graphitization is shown in Fig. 3 (bottom). The dashed gray spectrum is the subtraction of an unworn UNCD spectrum from the *HD* track spectrum. The result is similar to the spectrum from hydrogenated amorphous carbon [34] (Fig. 3, dashed black line), suggesting that some amount of amorphous carbon was created by wear. We performed a similar calculation to that done for graphite, instead using the hydrogenated amorphous carbon spectrum in Fig. 3 for the topmost layer. This analysis revealed that an amorphous carbon layer only  $0.25 \pm 0.01$  nm thick yields the same  $sp^2$  content found in the heavily modified region of track *HD*. Far less amorphous carbon is detected in all the other tracks, yet they have similar steady-state friction coefficients ( $\sim 0.02$ ) as the *HD* track. The UNCD in these tracks remains almost completely unaltered at the surface, with no graphitization or significant amorphization. We conclude that the much-discussed lubrication mechanism for diamond involving the formation of substantial graphitic or amorphous interfacial layers does not occur for UNCD under a broad range of conditions. This may be generalized to any diamond interface since UNCD possesses only slightly more  $sp^2$  bonding than larger-grained and single crystal diamond.

The mechanism of low friction supported by this spectroscopy is passivation of dangling bonds [1,3,4,35]. This is the first definitive spectroscopic evidence supporting the passivation hypothesis. This mechanism hinges on a balance between the processes of bond breaking during each sliding pass (which depends on contact stress, sliding rate, and temperature) and passivation by dissociative adsorp-

tion of gaseous species, in particular, water vapor (which depends on RH and reciprocation frequency [36,37]). Recent density functional theory calculations demonstrate the strong energetic favorability of H<sub>2</sub> and H<sub>2</sub>O dissociative passivation of dangling bonds on diamond [32]. With H<sub>2</sub>O, the dangling bonds become either -OH or -H terminated. Indeed, we have evidence that there is an increase of C—O and C=O bonding [Fig. 2(b)]. Results agree with other tribological studies, which infer that dissociative passivation either by water [3,5,24] or by H<sub>2</sub> [4,38–40] is responsible for the low friction and wear of diamond.

Funding was provided by Air Force Grant No. FA9550-05-1-0204 to R. W. C. and P. U. P. A. G. The ALS is supported by the DOE under Contract No. DE-AC02-05CH11231. Use of the Center for Nanoscale Materials was supported by the U.S. Department of Energy, Office of Science, Office of Basic Energy Sciences, under Contract No. DE-AC02-06CH11357. Part of this work was supported by DOE–Office of Science–Materials Science under Contract No. W-31-109-ENG-38. The authors acknowledge Dr. Schöll and Dr. Doran for help with PEEM II at the Advanced Light Source (ALS), Dr. O. Auciello from ANL for his help with the UNCD growth, and Dr. M. Hamilton for reviewing this manuscript.

---

\*Previously published as Gelsomina De Stasio.

- [1] M. N. Gardos and B. L. Soriano, *J. Mater. Res.* **5**, 2599 (1990).
- [2] A. Erdemir, G. R. Fenske, A. R. Krauss, D. M. Gruen, T. McCauley, and R. T. Csencsits, *Surf. Coat. Technol.* **120–121**, 565 (1999).
- [3] S. E. Grillo and J. E. Field, *J. Phys. D* **33**, 595 (2000).
- [4] M. N. Gardos and S. A. Gabelich, *Tribol. Lett.* **6**, 103 (1999).
- [5] H. I. Kim, J. R. Lince, O. L. Eryilmaz, and A. Erdemir, *Tribol. Lett.* **21**, 51 (2006).
- [6] A. Erdemir, O. L. Eryilmaz, and G. Fenske, *J. Vac. Sci. Technol. A* **18**, 1987 (2000).
- [7] L. Sun, Q. Wu, Y. Zhang, and W. Wang, *J. Mater. Res.* **14**, 631 (1999).
- [8] M. N. Gardos, *Tribol. Lett.* **2**, 173 (1996).
- [9] G. T. Gao, P. T. Mikulski, G. M. Chateaufneuf, and J. A. Harrison, *J. Phys. Chem. B* **107**, 11082 (2003).
- [10] A. V. Sumant, D. S. Grierson, J. E. Gerbi, J. Birrell, U. D. Lanke, O. Auciello, J. A. Carlisle, and R. W. Carpick, *Adv. Mater.* **17**, 1039 (2005).
- [11] A. R. Krauss *et al.*, *Diam. Relat. Mater.* **10**, 1952 (2001).
- [12] H. D. Espinosa and P. Bei, *J. Microelectromech. Syst.* **14**, 153 (2005).
- [13]  $1 \times 1$  cm<sup>2</sup> flats, and 3 mm diameter spheres.
- [14] X-PEEM measurements were performed using PEEM-II at the Advanced Light Source at Lawrence Berkeley National Laboratory.
- [15] S. Anders *et al.*, *Rev. Sci. Instrum.* **70**, 3973 (1999).
- [16] B. H. Frazer, B. Gilbert, B. R. Sonderegger, and G. De Stasio, *Surf. Sci.* **537**, 161 (2003).
- [17] D. S. Grierson *et al.*, *J. Vac. Sci. Technol. B* **25**, 1700 (2007).
- [18] P. L. Dickrell, S. B. Sinnott, D. W. Hahn, N. R. Raravikar, L. S. Schadler, P. M. Ajayan, and W. G. Sawyer, *Tribol. Lett.* **18**, 59 (2005).
- [19] The normal load, friction force, track position, and relative humidity were all recorded at a sampling rate of 1 kHz. RH was measured within  $\pm 0.1\%$  (DewPro MMY 2650).
- [20] A speed of 2.5 mm/s and a 600  $\mu$ m wear track length for 5000 cycles.
- [21] Using a Zygo New View 5010 scanning white light interferometer.
- [22]  $K = VF_N^{-1}d^{-1}$ , where  $K$  is the assumed linear wear rate,  $V$  the volume removed,  $F_N$  the applied load, and  $d$  the total sliding distance.
- [23] Other tests demonstrated that the run-in period progressively reduces with increasing RH and is eventually eliminated above a threshold RH between 1.0% and 5.0%.
- [24] K. Miyoshi, in *Proceedings of the Applied Diamond Conference 1995. Applications of Diamond Films and Related Materials: Third International Conference*, (NIST, Gaithersburg, MD, 1995), p. 493.
- [25] Using a Jobin Yvon LabRAM Confocal Raman Microscope with a 17 mW HeNe laser source.
- [26] J. Birrell, J. E. Gerbi, O. Auciello, J. M. Gibson, J. Johnson, and J. A. Carlisle, *Diam. Relat. Mater.* **14**, 86 (2005).
- [27] A. Erdemir, M. Halter, G. R. Fenske, C. Zuiker, R. Csencsits, A. R. Krauss, and D. M. Gruen, *Tribol. Trans.* **40**, 667 (1997).
- [28] Worn and unworn areas were imaged in the same field of view when possible. X-PEEM could not be performed on the spheres. No significant chemical differences compared to the flats were expected, and none were detected by Raman or interferometry.
- [29] J. Stöhr, *NEXAFS Spectroscopy* (Springer-Verlag, Berlin, Heidelberg, 1992).
- [30] R. Gago, I. Jimenez, and J. M. Albella, *Surf. Sci.* **482–485**, 530 (2001).
- [31] S. Osswald, G. Yushin, V. Mochalin, S. O. Kucheyev, and Y. Gogotsi, *J. Am. Chem. Soc.* **128**, 11635 (2006).
- [32] Y. Qi, E. Konca, and A. T. Alpas, *Surf. Sci.* **600**, 2955 (2006).
- [33] E. Gullikson, “X-Ray Interactions With Matter,” [http://henke.lbl.gov/optical\\_constants/](http://henke.lbl.gov/optical_constants/).
- [34] N. J. Mehta *et al.*, *Mater. Res. Soc. Symp. Proc.* **843**, 49 (2005).
- [35] Z. Feng, Y. Tzeng, and J. E. Field, *J. Phys. D* **25**, 1418 (1992).
- [36] P. L. Dickrell, W. G. Sawyer, and A. Erdemir, *J. Tribol.* **126**, 615 (2004).
- [37] P. L. Dickrell, W. G. Sawyer, J. A. Heimberg, I. L. Singer, K. J. Wahl, and A. Erdemir, *Trans. ASME J. Tribol.* **127**, 82 (2005).
- [38] S. V. Pepper, *J. Vac. Sci. Technol.* **20**, 643 (1982).
- [39] R. J. A. van den Oetelaar and C. F. J. Flipse, *Surf. Sci.* **384**, L828 (1997).
- [40] G. T. Gao, P. T. Mikulski, and J. A. Harrison, *J. Am. Chem. Soc.* **124**, 7202 (2002).